

Long Range Tensor Correlations in Charge and Parity Projected Fermionic Molecular Dynamics

Sonia Bacca*, Hans Feldmeier and Thomas Neff

Gesellschaft für Schwerionenforschung, Planckstr. 1, 64291 Darmstadt, Germany

Within the framework of Fermionic Molecular Dynamics a method is developed to better account for long range tensor correlations in nuclei when working with a single Slater determinant. Single-particle states with mixed isospin and broken parity build up an intrinsic Slater determinant which is then charge and parity projected. By minimizing the energy of this many-body state with respect to the parameters of the single-particle states and projecting afterwards on angular momentum ground state energies are obtained that are systematically lower than corresponding Hartree-Fock results. The realistic Argonne V18 potential is used and short range correlations are treated with the Unitary Correlation Operator Method. Comparison with exact few-body calculations shows that in ${}^4\text{He}$ about one fifth of the correlation energy due to long-range correlations are accounted for. These correlations which extend over the whole nucleus are visualized with the isospin and spin-isospin density of the intrinsic state. The divergence of the spin-isospin density, the source for pion fields, turns out to be of dipole nature.

PACS numbers: 21.60.-n, 21.60.De, 21.10.Hw, 21.30.Fe

I. INTRODUCTION

Despite the undeniable successes of mean field models a more microscopic view on the structure of atomic nuclei reveals correlations among the nucleons of various kinds. These are induced by realistic nucleon-nucleon interactions and cannot be represented by a single Slater determinant in a mean field picture.

Impressive progress has been made in the derivation of the nuclear interaction, one of the latest achievements being the nucleon-nucleon (NN) forces and consistent many-nucleon forces developed with chiral perturbation theory [1, 2]. Furthermore, a number of other nuclear potentials exist, like the semi-phenomenological Argonne V18 potential (AV18) [3], which reproduce the experimental NN phase shifts with high precision. Common to the realistic NN forces mentioned before are two general features: (i) they are strongly repulsive at very small distances, preventing nucleons to stay close together, which induces short-range repulsive radial correlations among them; (ii) they contain a tensor force component, such that the nucleon pair feels a force which depends on their spin orientation with respect to the relative distance. This induces further short and long range tensor correlations among nucleons.

It is well known that a Slater determinant (antisymmetrized product state) cannot represent such correlations. Models that use a Slater determinant basis need very large many-body Hilbert spaces to represent these correlations. Therefore in the no-core shell model (NSCM) [4] the unitary Lee-Suzuki transformation is incorporated to treat the short range part of the Hamiltonian that scatters to very high lying oscillator shells

and thus helps to improve convergence and to reduce the dimensions of the Hilbert space.

Another possible solution to overcome the problems caused by the short-range correlations is the Unitary Correlation Operator Method (UCOM) [5, 6, 7]. A unitary correlator $\mathcal{C} = \mathcal{C}_\Omega \mathcal{C}_r$ is devised to imprint explicitly the short range tensor correlations, by means of \mathcal{C}_Ω , and radial correlations, by \mathcal{C}_r , into the uncorrelated Slater determinant basis.

However, tensor correlations are not only of short range like the radial repulsive correlations, but contain parts of long-range nature originating from the one pion exchange, exemplified e.g. by the large extension of the D -wave component of the deuteron wave function. Therefore, even when using the UCOM approach long-range correlations need to be incorporated by configuration mixing in the Hilbert space. In case of many-body methods based on an expansion of the states in terms of a complete set of basis states one is in principle able to account for all kind of correlations, provided that convergence in the expansion is reached. But when working with a low-momentum basis, like with just one or few Slater determinant states, the incapability of describing long-range correlations in nuclei still constitutes a big limitation.

In this work, we would like to address the general problem of how to account for long-range tensor correlations within a restricted Slater determinant basis. We propose a method, which follows ideas presented by Ikeda, Sugimoto and Toki published in a series of papers [9, 10, 11, 12, 13] to allow proton and neutron states to mix at the single-particle level and then project the many-body state on good charge and parity. We introduce additional variational degrees of freedom in the Fermionic Molecular Dynamics (FMD) framework which allow for the possibility that the isospin of a nucleon can point in any direction in isospin space and not just in the

*present address: TRIUMF, 4004 Wesbrook Mall, Vancouver B.C., V6T 2A3, Canada

proton or neutron direction.

The paper is organized as follows. In Sec. II the theoretical background is set: an overview of the FMD and of its extension and the used effective interaction are presented. In Sec. III results are shown and conclusions are finally drawn in Sec. IV.

II. THEORETICAL OVERVIEW

A. Fermionic Molecular Dynamics

In the following we will briefly introduce the Fermionic Molecular Dynamics (FMD) approach and the generalization of the FMD wave functions to mixed charge states. In FMD [14, 15, 16, 17, 18, 19] the many-body Hilbert space is spanned by non-orthogonal many-body basis states which are given by antisymmetrized products of single particle states, as

$$|Q\rangle = \mathcal{A}\left(|q_1\rangle \otimes \cdots \otimes |q_A\rangle\right). \quad (1)$$

\mathcal{A} is the antisymmetrization operator and $|q_k\rangle$ denote the single-particle states which are linear combinations of Gaussian wave packets localized in phase-space, with variable spin orientation $|\chi\rangle$ and the generalized isospinor $|\xi\rangle$,

$$\langle \vec{x} | q \rangle = \sum_i c_i \exp\left\{-\frac{(\vec{x} - \vec{b}_i)^2}{2a_i}\right\} \otimes |\chi_i\rangle \otimes |\xi_i\rangle. \quad (2)$$

Each Gaussian wave packet is parameterized in terms of a complex vector \vec{b}_i , indicating the mean position and momentum and a complex width parameter a_i , which can be different for each Gaussian, in contrast to the AMD approach [20] where the widths are real and common for all nucleons.

The spinor is parameterized via two complex components for spin-up and spin-down

$$|\chi_i\rangle = \chi_i^\uparrow |\uparrow\rangle + \chi_i^\downarrow |\downarrow\rangle \quad (3)$$

allowing for all orientations of the spin. Analogously the generalized isospin part $|\xi_i\rangle$ describes a linear superposition of proton $|p\rangle$ and neutron $|n\rangle$

$$|\xi_i\rangle = \xi_i^p |p\rangle + \xi_i^n |n\rangle \quad (4)$$

so that a nucleon can adopt any “direction” in isospin space. In former applications of FMD $|\xi\rangle$ was either a proton $|p\rangle$ or a neutron state $|n\rangle$.

This generalization introduces charge mixing in the single-particle and many-body space. In a description, where the degrees of freedom are only nucleons and the charged mesons do not appear explicitly, the charge carried by the nucleons is a sharp quantum number. The many-body state $|Q\rangle$ however breaks the symmetry with

respect to isospin rotations around the 3-axis. Therefore one has to project on the desired charge number corresponding to the eigenvalue M_T of the third component of the total isospin

$$\tilde{T}^{(3)} = \sum_{k=1}^A \tilde{t}^{(3)}(k) = \frac{1}{2} \sum_{k=1}^A \tilde{\tau}^{(3)}(k). \quad (5)$$

This is achieved by the charge projection operator [23]

$$\tilde{P}^{M_T} = \frac{1}{A} \sum_{n=1}^A \exp\left\{i\frac{2\pi n}{A}(\tilde{T}^{(3)} - M_T)\right\}. \quad (6)$$

Thus, the charge projected state, can be written as a superposition of Slater determinants $|Q^{(n)}\rangle$ obtained by rotating the single determinant $|Q\rangle$ in isospin space about an angle $2\pi n/A$:

$$\begin{aligned} |Q; M_T\rangle &= \tilde{P}^{M_T} |Q\rangle \\ &= \frac{1}{A} \sum_{n=1}^A e^{-i\frac{2\pi n}{A}M_T} |Q^{(n)}\rangle. \end{aligned} \quad (7)$$

The following simple example shows that the projection of a two-body product state with mixed charges results in correlated states with good isospin. From the product states of two nucleons

$$\begin{aligned} \left(|p\rangle \pm |n\rangle\right) \otimes \left(|p\rangle + |n\rangle\right) &= \\ |p\rangle \otimes |p\rangle \pm |n\rangle \otimes |n\rangle &+ \\ + \left(|p\rangle \otimes |n\rangle \pm |n\rangle \otimes |p\rangle\right) & \end{aligned} \quad (8)$$

one can project out all 4 components with isospin $T=1$ and 0 including the $M_T=0$ two-body states

$$|T=1, M_T=0\rangle = \frac{1}{\sqrt{2}} \left(|p\rangle \otimes |n\rangle + |n\rangle \otimes |p\rangle\right) \quad (9)$$

$$|T=0, M_T=0\rangle = \frac{1}{\sqrt{2}} \left(|p\rangle \otimes |n\rangle - |n\rangle \otimes |p\rangle\right) \quad (10)$$

which are correlated and cannot be written as a product of two single-particle states.

As the lightest charged meson, the pion, is of pseudoscalar nature with a negative intrinsic parity it may carry besides charge also parity from one nucleon to the other. Therefore we also allow for parity breaking in the FMD state, which simply means that the parameters \vec{b}_i are not the same for all nucleons, and restore it by projection on good parity $\pi = \pm 1$ with the projection operator

$$\tilde{P}^\pi = \frac{1}{2} (\mathbb{1} + \pi \tilde{\Pi}), \quad (11)$$

where $\tilde{\Pi}$ is the parity operator.

In order to see in how far Slater determinants, that break charge and parity, can represent long range correlations induced by the exchange of pions variational

calculations are performed. We minimize the energy

$$\frac{\langle Q; \pi, M_T | \underline{H} | Q; \pi, M_T \rangle}{\langle Q; \pi, M_T | Q; \pi, M_T \rangle} = \frac{\langle Q | \underline{H} \underline{P}^{M_T} \underline{P}^\pi | Q \rangle}{\langle Q | \underline{P}^{M_T} \underline{P}^\pi | Q \rangle} \quad (12)$$

of the charge and parity projected FMD state

$$| Q; \pi, M_T \rangle = \underline{P}^{M_T} \underline{P}^\pi | Q \rangle \quad (13)$$

with respect to all single-particle parameters contained in the single Slater determinant $| Q \rangle$.

As the intrinsic Hamiltonian \underline{H} commutes with $\underline{\Pi}$ and \underline{T}_3 one has to project only the ket-state so that the number of terms in the energy (12) is reduced.

The correlated many-body state $| Q; \pi, M_T \rangle$ that results from the minimization of the energy (12) in general breaks rotational and translational symmetry. Therefore we project after the variation on good angular momentum and center of mass momentum zero [18, 19]:

$$| Q; J^\pi, MK, M_T \rangle = \underline{P}_{MK}^J \underline{P}_{CM} | Q; \pi, M_T \rangle. \quad (14)$$

Throughout this paper we consider only energies of $J^\pi = 0$ states so that $K = M = 0$. All energies are calculated as expectation values of the intrinsic Hamiltonian $\underline{H} = \underline{T} - \underline{T}_{cm} + \underline{V}$ where the center of mass kinetic energy has been subtracted:

$$E(0^+) = \frac{\langle Q | \underline{H} | Q; J^\pi = 0^+, 00, M_T \rangle}{\langle Q | Q; J^\pi = 0^+, 00, M_T \rangle}. \quad (15)$$

It would be of course desirable to first restore all symmetries of the Hamiltonian and then do the variation with respect to the single-particle parameters contained in $| Q \rangle$. However, angular momentum projection requires the superposition of a few hundred rotated states, which is numerically very costly. Therefore we do a variation after charge and parity projection and project on angular momentum and CM-momentum zero after variation.

B. Unitary Correlation Operator Method

Realistic nucleon nucleon interactions, like the chiral forces or the Argonne V18 potential, that reproduce the phase shifts and the deuteron properties, induce strong short range correlations. The repulsive core prevents two nucleons from getting too close. In the $T=0$ channel the tensor force induces correlations by aligning the spins of two interacting nucleons along their distance vector. Both correlations cannot be represented by Slater determinants. Even though the Slater determinants of a shell model basis form a complete set, diagonalization of a realistic Hamiltonian in the 4-body space shows that convergence cannot be reached in any tractable shell model space [8]. Thus many-body Slater determinants are an

inadequate representation for these short ranged correlations. In fact the no-core shell model employs the Lee-Suzuki transformation of the Hamiltonian which improves the convergence dramatically.

Here we will use the Unitary Correlation Operator Method (UCOM) to take care of the short range correlations. The reason is that an effective interaction to be used in the FMD Hilbert space has to be represented in an operator form, rather than in terms of matrix elements as is the case for a Lee-Suzuki transformation or a G-matrix. UCOM provides both representations so that we can compare with no-core shell model results.

The concept of UCOM [5, 6, 7] consists in treating explicitly the strong short range correlations induced by the hard core and the short range part of the tensor force by a state independent unitary transformation, while the long range correlations have to be represented by the many-body states spanning the Hilbert space. When the correlation operator is applied to an initial Hamiltonian, a phase-shift equivalent correlated interaction is obtained. The correlated Hamiltonian is defined via a similarity transformation

$$\begin{aligned} \hat{H} &= \underline{C}_r^{-1} \underline{C}_\Omega^{-1} \underline{H}_{\text{initial}} \underline{C}_\Omega \underline{C}_r \\ &= \underline{T} - \underline{T}_{cm} + \underline{V}_{\text{UCOM}} + 3\text{-body} + \dots \end{aligned} \quad (16)$$

where \underline{C}_r and \underline{C}_Ω are the unitary central and tensor correlation operators, respectively. \underline{C}_r shifts pairs of nucleons radially away from each other whenever their distance is so small that they would be inside the repulsive core. \underline{C}_Ω aligns nucleon pairs with $T=0$ and $S=1$ along the direction of their total spin so that the typical tensor correlations known from the deuteron are imprinted into the many-body state. Different from the radial correlations induced by the short ranged repulsion, the tensor interaction mediated by the exchange of pions, the lightest of all mesons, induces long range correlations. In order to keep the effect of the induced many-body interactions small one restricts the range of the action of the tensor correlation operator \underline{C}_Ω and represents the long range part of the tensor correlations with the many-body state (see Ref. [8] for details).

The two-body part of the correlated Hamiltonian (16) is used as an effective intrinsic Hamiltonian

$$\underline{H} = \underline{T} - \underline{T}_{cm} + \underline{V}_{\text{UCOM}} \quad (17)$$

that is applicable in low momentum Hilbert spaces. The effective interaction $\underline{V}_{\text{UCOM}}$ is phase shift equivalent to the initial realistic interaction. Moreover different realistic potentials, like Bonn A, Nijmegen or Argonne V18, lead to practically the same $\underline{V}_{\text{UCOM}}$. In FMD the effective potential needs to be given in operator representation and not as momentum space matrix elements for the different partial waves. $\underline{V}_{\text{UCOM}}$ can easily be obtained in operator form if the initial interaction is given in terms of operators. Therefore we use in this publication the Argonne V18 potential (AV18) as initial potential because it is already in operator form.

For a better understanding of the results let us first consider in somewhat more detail how the tensor correlator \mathcal{C}_Ω acts. Any operator that depends only on the distance r between two nucleons is invariant under actions of the tensor correlator

$$\mathcal{C}_\Omega^{-1} V(r) \mathcal{C}_\Omega = e^{+ig_\Omega} V(r) e^{-ig_\Omega} = V(r), \quad (18)$$

because the tensorial generator

$$g_\Omega = \vartheta(r) \frac{3}{2} \left((\vec{p}_\Omega \cdot \vec{\sigma}_1)(\vec{r} \cdot \vec{\sigma}_2) + (\vec{r} \cdot \vec{\sigma}_1)(\vec{p}_\Omega \cdot \vec{\sigma}_2) \right) \quad (19)$$

commutes with $\vec{r} = |\vec{r}|$. The reason is that the so called orbital momentum \vec{p}_Ω , defined as the component of the relative momentum perpendicular to \vec{r} ,

$$\vec{p}_\Omega = \vec{p} - p_r \frac{\vec{r}}{r}, \quad (20)$$

commutes with \vec{r} . The correlation function $\vartheta(r)$ defines the strength of the transformation as a function of the distance between an $S=1$ nucleon pair.

In the following we shall use different $\vartheta(r)$ (displayed in Fig. 1) with varying range characterized by the range parameter $I_\vartheta = \int dr r^2 \vartheta(r)$.

When applying the tensor correlator to the tensor interaction

$$V_T(r) \mathcal{S}_{12} = V_T(r) \left(\frac{3}{r^2} (\vec{r} \cdot \vec{\sigma}_1)(\vec{r} \cdot \vec{\sigma}_2) - (\vec{\sigma}_1 \cdot \vec{\sigma}_2) \right) \quad (21)$$

it is unitarily “rotated” into a reduced tensor \tilde{V}_T , a central \tilde{V}_C , and a spin-orbit \tilde{V}_{LS} component, plus some other terms which are negligibly small.

$$\begin{aligned} \mathcal{C}_\Omega^{-1} V_T(r) \mathcal{S}_{12} \mathcal{C}_\Omega &= \tilde{V}_T + \tilde{V}_C + \tilde{V}_{LS} + \dots \quad (22) \\ &= e^{-3\vartheta(r)} V_T(r) \mathcal{S}_{12} \\ &+ 2(1 - e^{-3\vartheta(r)}) V_T(r) (3 + \vec{\sigma}_1 \cdot \vec{\sigma}_2) \\ &+ 6(1 - e^{-3\vartheta(r)}) V_T(r) \vec{l} \cdot \vec{s} \\ &+ \dots \end{aligned}$$

In Eq. (22) one readily sees that the induced central force \tilde{V}_C increases if the correlation function $\vartheta(r)$ increases. Thus with larger range of the tensor correlator more strength goes to the central and spin-orbit interaction. One should keep in mind that the correlation function $\vartheta(r)$ is different for isospin $T=0$ and $T=1$, see Ref. [6] and that there are also contributions from the correlated kinetic energy $\mathcal{C}_\Omega^{-1} T \mathcal{C}_\Omega$, the spin orbit force $\mathcal{C}_\Omega^{-1} \vec{l} \cdot \vec{s} \mathcal{C}_\Omega$ and possibly other terms in the interaction.

Eq. (22) also gives finally an explanation why in most textbooks after the discussion of the deuteron with its quadrupole moment and the mandatory tensor force the tensor interaction disappears in the following chapters

on mean-field theories like Hartree-Fock or simple shell-model pictures. The reason is that those calculations can be performed without the tensor force using only central and spin-orbit interactions that are fitted to energies and other properties of the many-body system. The success of these models does not imply that in finite nuclei or nuclear matter the tensor force is not important. By fitting the parameters of the interaction one has effectively moved the correlation energy of the tensor into central and spin-orbit interactions. However, the resulting effective interactions are not phase-shift equivalent any longer, V_{UCOM} is. Furthermore, the uncorrelated many-body Slater determinants do not possess the tensor correlations anymore that are existent in reality and can be observed for example in the high momentum part of the momentum distribution of the nucleons [6].

III. RESULTS

In the following subsections we study in how far long range correlations originating from the tensor interaction can be represented by a charge and parity projected Slater determinant. For that the realistic AV18 interaction is used and the results are compared to exact solutions for the 4-body system ${}^4\text{He}$.

In subsection III C we use a phenomenological interaction that is not based on a realistic nucleon nucleon force to illustrate that fitting interaction parameters to a specific nucleus may be misleading when drawing conclusions about the strength of correlations.

A. Correlation energies

In this section we investigate how the induced correlations are accounted for by breaking charge and parity in each single-particle state as a function of the strength of the tensor component of the nucleon-nucleon interaction. In order to get a fair judgement we use the realistic effective interaction V_{UCOM} which is derived from the AV18 potential. The strength of its tensor component depends on the range I_ϑ of the tensor correlator. This range corresponds to the cutoff in momentum space in the $V_{\text{low } k}$ -approach [6, 27]. For all values of I_ϑ the effective interaction V_{UCOM} is phase shift equivalent to the original realistic interaction. It should be noted that for different I_ϑ all parts of the V_{UCOM} potential change accordingly under the similarity transformation (16) and not just the tensor part (see also Eq. (22)).

We calculate the ground state energy of ${}^4\text{He}$ in three different ways using the same effective Hamiltonian (17) for different I_ϑ .

First we minimize the energy $\langle Q | \tilde{H} | Q \rangle / \langle Q | Q \rangle$ with respect to all FMD parameters contained in Q without any projection. The FMD single-particle states $|q_k\rangle$ contain two Gaussians, see Eq. (2). The results are labelled HF as this variation corresponds to a Hartree-Fock

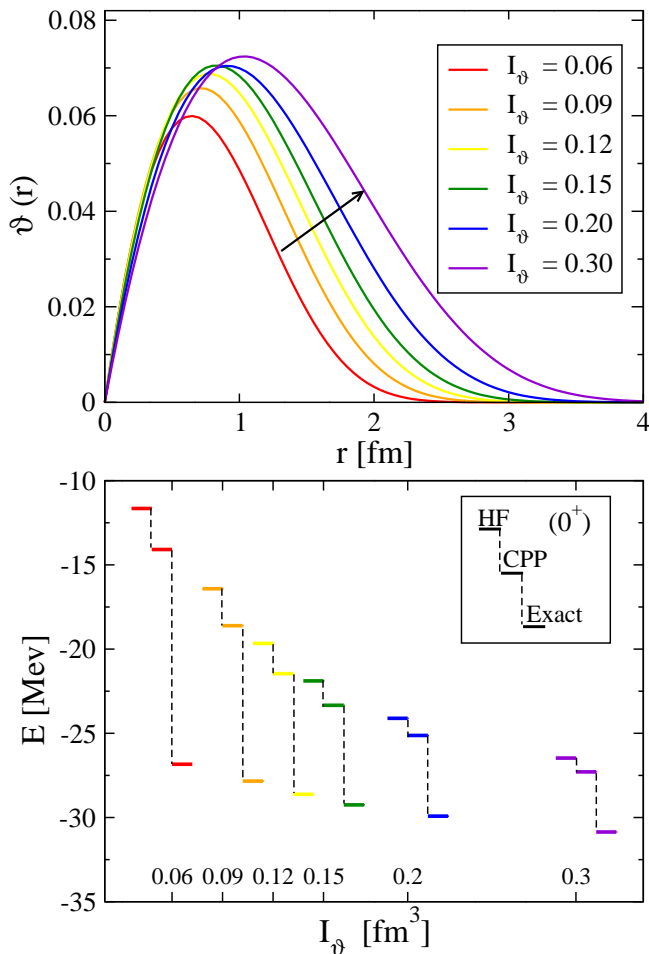


FIG. 1: (Color online) Upper panel: tensor correlation functions $\vartheta(r)$ with increasing range I_ϑ (arrow). Lower panel: ground state energies of ${}^4\text{He}$ calculated with the HF and CPP states compared to exact results. The correlation functions shown in the upper panel are used.

minimization. Second we minimize the energy (12) of the charge and parity projected FMD Slater determinant (13), labelled CPP.

After that an angular momentum and CM projection is applied to the HF and CPP state, see Eq. (14). The HF state has already $J^\pi = 0^+$ and $M_T = 0$ but the CPP state has no good angular momentum. The resulting energies (15) are compared to the exact results of no-core shell model and hyperspherical harmonics calculations.

In order to study the effects of different tensor strengths in the Hamiltonian we vary the range of the tensor correlator in the $S = 1$, $T = 0$ channel, which according to Eq. (22) moves strength from the tensor to the central part. This has the advantage that we are always using phase-shift equivalent potentials. In the upper part of Fig. 1 we display the correlation functions employed. They differ in range which we quantify by the range parameter I_ϑ .

In the lower part of Fig. 1 we present the binding en-

ergies of ${}^4\text{He}$ obtained with the V_{UCOM} potential for different I_ϑ in the three variational Hilbert spaces as explained before. The range $I_\vartheta = 0.09 \text{ fm}^3$ corresponds to the standard choice where V_{UCOM} reproduces within 0.5 MeV both the ${}^4\text{He}$ and ${}^3\text{He}$ binding energies. This interaction has been used for many applications, ranging from few- to many-body problems [8, 21, 24, 25, 26]. The range $I_\vartheta = 0.09 \text{ fm}^3$ is optimal in the sense that the net contribution from 3-body forces is minimized [8].

The exact results in Fig. 1 show that ranges smaller than $I_\vartheta = 0.09 \text{ fm}^3$ lead to underbinding with respect to the experimental energy of -28.3 MeV (like for most realistic potentials). On the other hand tensor correlators with ranges larger than $I_\vartheta = 0.09 \text{ fm}^3$ induce 3- and 4-body interactions in the correlated Hamiltonian \hat{H} , Eq. (16), which are on average repulsive but not included here. A similar kind of overbinding was obtained with $V_{\text{low } k}$ for cutoffs $\sim 1.6 \text{ fm}^{-1}$ [27].

The first result to be observed in Fig. 1 is the decreasing difference between the HF energy and the exact result when the range I_ϑ of the tensor correlator is enlarged. This can be understood if one keeps in mind that the HF state of ${}^4\text{He}$ is a pure $(0s)^4$ configuration so that the tensor interaction cannot contribute. All binding comes from the central part of the interaction. According to Eq. (22) increasing the correlation strength implies that the induced central part of the correlated tensor interaction (22) in the $S = 1$ $T = 0$ channel increases and binding energy is gained, while the long range part of the tensor force, not seen by the HF state, is reduced. The difference between the HF and the exact energy is the correlation energy which is due to the interaction induced correlations present in the exact many-body state but absent in the HF Slater determinant.

The exact results obtained in an “unrestricted” Hilbert space show much less variation as function of I_ϑ because there the long range correlations are represented in the many-body state even for small I_ϑ . If we would include the induced 3- and 4-body potentials the exact energy would not depend on I_ϑ because the transformation would then be unitary even in the many-body space.

An important finding is that, although the variational manifold $\{Q\}$ includes the new isospin mixing degrees of freedom, the Hartree-Fock (HF) minimum does not make use of them. All ξ_i^p and ξ_i^n are either 0 or 1, so that the Hartree-Fock state is already an eigenstate of charge. It turns out to be also an eigenstate of angular momentum and parity ($J^\pi = 0^+$).

This changes when the variation is performed after charge and parity projection. Now the ξ_i^p and ξ_i^n parameter assume values different from 0 or 1. As Fig. 1 shows, the charge and parity projected state (CPP) can represent part of the long range correlations leading to a correlation energy of about 20% the full correlation energy.

In Table I the expectation values of the total Hamiltonian, the kinetic energy, the interaction energy and the tensor part of the correlated interaction V_{UCOM} are

TABLE I: Expectation values of different terms of the Hamiltonian for the ${}^4\text{He}$ $J^\pi = 0^+$ ground state. The variation of single-particle states is performed for Hartree-Fock (HF), Parity Projected (PP) and Charge and Parity Projected (CPP) intrinsic Slater determinants. V_{UCOM} with tensor correlator range $I_\vartheta = 0.09 \text{ fm}^3$ is used. Numerical values are in MeV.

	HF[0^+]	PP [0^+]	CPP [0^+]
$\langle \tilde{H} \rangle$	-16.42	-17.51	-18.61
$\langle \tilde{T} \rangle$	50.25	51.56	57.93
$\langle \tilde{V} \rangle$	-66.68	-69.07	-76.54
$\langle \tilde{V}_T \rangle$	0.00	-1.35	-4.59

listed. The HF state has zero tensor energy and the smallest kinetic energy, while the CPP state contains correlations that yield about -2.2 MeV more binding. These consist of 7.7 MeV kinetic energy counterbalanced by -9.9 MeV additional potential energy. Out of that the tensor contributes -4.6 MeV . The rest originates from other parts. The rather large increase in kinetic energy is partly due to the fact that in the CPP minimum the two Gaussians in the single-particle states are displaced from each other, thus break parity and include higher angular momenta. Therefore the spatial and spin parts are different in the CPP minimum and the HF minimum.

It is interesting to note that a variation after parity projection (PP) already takes into account part of the correlations as can be seen from the center column of Table I. One should also keep in mind that with respect to an uncorrelated Slater determinant a by far larger amount of correlation energy resides in the short range tensor correlations which are treated here by the Unitary Correlation Operator Method (UCOM). These short range correlations are so strong that they even cannot be properly accounted for in a very large scale shell model basis, not to mention a single Slater determinant.

The effects are not as pronounced if one restricts the single-particle states to one Gaussian. Adding the second Gaussian is essential in describing tensor correlations, as it allows to add higher angular momenta components to the single-particle wave functions.

One should pay attention to the fact that additional correlations in the many-body state that are induced by the two-body interaction give an attractive contribution from the potential but at the same time the kinetic energy rises. For example tensor correlations imply admixtures of higher angular momenta and thus more kinetic energy. Hence the correlation energy is the result of a subtle interplay between enhanced kinetic energy and increased attractive potential energy.

The ground state energies labelled “Exact” are calculated within the no-core shell model (NCSM) using the translationally invariant harmonic oscillator formulation of Petr Navrátil [29] and the hyperspherical harmonics (HH) approach developed by Nir Barnea [30, 31]. The latter method has been applied to the calculation of ex-

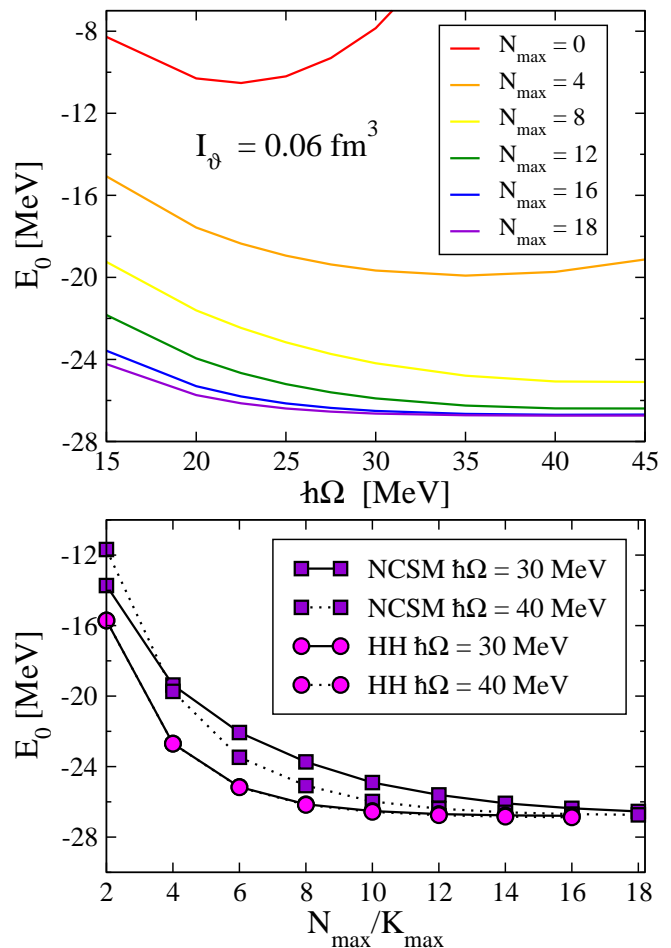


FIG. 2: (Color online) Convergence patterns for the NCSM calculations with the UCOM potential for $I_\vartheta = 0.06 \text{ fm}^3$: the ground state energy of ${}^4\text{He}$ is plotted as a function of the oscillator parameter $\hbar\Omega$ for different model space sizes (upper panel). Comparison of the NCSM and HH convergence as a function of N_{max} and K_{max} , respectively, for fixed $\hbar\Omega$ (lower panel).

act electroweak reactions on light nuclei mainly with local interactions [32, 33, 34, 35, 36, 37, 38]. Recently it has been extended to use interactions represented in harmonic oscillator (HO) states (see e.g. Refs. [26, 39]). The HH approach is equivalent to the NCSM, but makes use of HH functions instead of HO eigenstates. The label “Exact” is meant in the sense that one systematically enlarges the Hilbert space and controls the convergence to approach the final many-body state which should contain all kind of correlations induced by the interaction.

Convergence patterns for the NCSM calculations for a specific value of $I_\vartheta = 0.06 \text{ fm}^3$ are shown in Fig. 2. For a given size of the model space, characterized by the maximum oscillator quantum number N_{max} , the ground state energy is plotted as a function of the oscillator parameter $\hbar\Omega$. Convergence, resulting in a flat energy curve over a significant range of oscillator parameters, can be

TABLE II: Exact ground state energies (in MeV) of ${}^4\text{He}$ for different ranges of the tensor correlator in UCOM, calculated with the NCSM and HH approaches.

I_ϑ [fm 3]	0.06	0.09	0.12	0.15	0.20	0.30
NCSM	-26.80(3)	-27.80(3)	-28.62(9)	-29.26(13)	-29.86(10)	-30.70(6)
HH	-26.84(6)	-27.84(7)	-28.62(7)	-29.25(8)	-29.92(10)	-30.86(10)

obtained already with $N_{\text{max}} = 18$. The energy gained compared with the results obtained with more moderate model spaces can be attributed to the residual long range correlations not described via the UCOM.

In Fig. 2 we also compare the convergence of the HH and NCSM calculations for two fixed values of $\hbar\Omega$ as a function of the K_{max} parameter, which is for the HH the analog to N_{max} for the NCSM. As already pointed out in Refs. [26] and [40] the convergence of HH is superior to the one of the NCSM, since no $\hbar\Omega$ dependence is observed even for small Hilbert spaces. Therefore we employ an exponential fit of the NCSM energies as a function of N_{max} (for fixed $\hbar\Omega$) to extrapolate to infinite dimensions. The further energy gain is of the order of 50 – 100 keV. The energies obtained for different values of the tensor correlator volume I_ϑ used in the UCOM are shown in Table II. The NCSM and HH results nicely agree with each other within the error bars.

The small difference of about 0.5 MeV we find in our exact calculations for $I_\vartheta = 0.09$ fm 3 with respect to the values previously published in Refs. [8] with the NCSM and [26] with HH for the same I_ϑ is related to some minor differences of the potential used. They originate from the fact that in this paper we adopt a V_{UCOM} potential in operator representation which is suited for the FMD code. This implies a truncation of the Baker-Campbell-Hausdorff expansion (for details see Ref. [8]), not needed if one correlates directly the two-body states.

Here, we would like to stress again that the exact approaches make use of thousands of basis states to reach convergence in energy, whereas with our improved FMD wave function we vary the parameters of a single Slater determinant projected on charge and parity.

B. Pseudo-scalar iso-vector correlations

A single Slater determinant can usually not represent correlations except those induced by the Pauli principle. However, if the Slater determinant represents an intrinsic state the situation is different. The physical state that has the same symmetries as the Hamiltonian is obtained by means of projection on angular momentum, parity and, as in our case, on charge. It is in general not a single Slater determinant but a superposition of many, see Eqs. (13, 14), with the restriction that all these Slater determinants are generated from a single one by means of rotations, parity inversion or rotation in isospin space.

A well known example for long range correlations in

nuclei are intrinsically deformed nuclei where out of one deformed intrinsic state one projects a whole rotational band.

The intrinsic state for ${}^4\text{He}$ obtained in this paper by variation after parity and charge projection shows a pronounced long range correlation in the spin isospin degrees of freedom. To elaborate on that let us consider the exchange of the pseudo-scalar iso-vector pion.

In all realistic nucleon-nucleon interactions the one-pion exchange is responsible for the long range tail of the potential. This part is not affected by the unitary correlator \mathcal{C}_Ω which is of short range. The induced long range correlations should therefore be represented by the many-body state.

The vertex describing the interaction of a nucleon field $N(\mathbf{x})$ with a pion field $\Phi_\pi^{(i)}(\mathbf{x})$ has in pseudo-vector coupling the following form

$$\mathcal{L}_{N\pi}(\mathbf{x}) = -\frac{g_\pi}{2M} \sum_{i=1}^3 \bar{N}(\mathbf{x}) \gamma^5 \gamma_\mu \tau^{(i)} N(\mathbf{x}) \partial^\mu \Phi_\pi^{(i)}(\mathbf{x}), \quad (23)$$

where $\tau^{(i)}$, $i = 1, 2, 3$ denote the Pauli matrices in isospin space.

$$\tau^{(1)} = \begin{pmatrix} 0 & 1 \\ 1 & 0 \end{pmatrix}, \quad \tau^{(2)} = \begin{pmatrix} 0 & -i \\ i & 0 \end{pmatrix}, \quad \tau^{(3)} = \begin{pmatrix} 1 & 0 \\ 0 & -1 \end{pmatrix} \quad (24)$$

In the stationary case the three components of the pion field $\Phi_\pi^{(i)}(\vec{x})$ satisfy the time-independent Klein-Gordon equation

$$(-\nabla^2 + m_\pi^2) \Phi_\pi^{(i)}(\vec{x}) = \frac{g_\pi}{M} \vec{\nabla} \cdot \vec{S}^{(i)}(\vec{x}), \quad (25)$$

where the source term is the divergence of the nuclear isospin current density

$$\vec{S}^{(i)}(\vec{x}) = \frac{1}{2} \bar{N}(\vec{x}) \gamma^5 \vec{\gamma} \tau^{(i)} N(\vec{x}). \quad (26)$$

After a non-relativistic reduction to leading order $\vec{S}^{(i)}(\vec{x})$ becomes the one-body spin-isospin density of the nuclear many-body system

$$\vec{S}^{(i)}(\vec{x}) = \frac{1}{2} \sum_{k=1}^A \delta^3(\vec{x} - \vec{r}(k)) \vec{\sigma}(k) \tau^{(i)}(k). \quad (27)$$

The relation with the physical pion fields are

$$\begin{aligned}\pi^+(\vec{x}) &= \frac{1}{\sqrt{2}}(\Phi_\pi^{(1)}(\vec{x}) + i\Phi_\pi^{(2)}(\vec{x})) \\ \pi^-(\vec{x}) &= \frac{1}{\sqrt{2}}(\Phi_\pi^{(1)}(\vec{x}) - i\Phi_\pi^{(2)}(\vec{x})) \\ \pi^0(\vec{x}) &= \Phi_\pi^{(3)}(\vec{x})\end{aligned}\quad (28)$$

The (3)-component $\vec{S}^{(3)}(\vec{x})$ is the difference between the proton and neutron spin density at position \vec{x} and $\vec{\nabla} \cdot \vec{S}^{(3)}(\vec{x})$ is the pseudo-scalar iso-vector source density for the π^0 field, while $\vec{\nabla} \cdot \vec{S}^{(1)}(\vec{x})$ and $\vec{\nabla} \cdot \vec{S}^{(2)}(\vec{x})$ are the sources for π^\pm fields.

In Fig. 3 various intrinsic densities are displayed as a function of x and y at the plane $z = 0$. All densities are calculated with the parity projected intrinsic state

$$|Q; +\rangle := \tilde{P}^{\pi=+1} |Q\rangle \quad (29)$$

that was obtained by minimizing the energy after parity and charge projection (CPP), cf. Eq. (12).

Before we come to the spin-isospin density that is related to the pion fields we show in Fig. 3 the proton and neutron densities for point-like nucleons. Both are equal up to very small deviations caused by the Coulomb interaction. This means that the isospin density $\rho_\tau^{(3)}(\vec{x}) = \rho_p(\vec{x}) - \rho_n(\vec{x})$ in the isospin (3)-direction is zero. However, the isospin density

$$\rho_\tau^{(1)}(\vec{x}) = \frac{\langle Q; + | \sum_{k=1}^A \delta^3(\vec{x} - \vec{r}(k)) \tilde{\mathcal{T}}^{(1)}(k) | Q; + \rangle}{\langle Q; + | Q; + \rangle} \quad (30)$$

in the (1)-direction orthogonal to the proton/neutron (3)-direction assumes a non-zero value. As seen in Fig. 3 this density is of quadrupole type. The intrinsic state $|Q; +\rangle$ is apparently not an eigenstate of $\tilde{T}^{(3)}$ and its new degrees of freedom, ξ^p, ξ^n , that allow to mix protons and neutrons, are responsible for this density. The charge and parity projected state $|Q; \pi = +1, M_T = 0\rangle$ has (like the Hartree-Fock state) again a vanishing isospin-(1) density.

The lower panels in Fig. 3 display the spin-isospin density

$$\vec{S}^{(1)}(\vec{x}) = \frac{\langle Q; + | \vec{\tilde{S}}^{(1)}(\vec{x}) | Q; + \rangle}{\langle Q; + | Q; + \rangle} \quad (31)$$

and its divergence $\vec{\nabla} \cdot \vec{S}^{(1)}(\vec{x})$ which is the source density for the $\Phi_\pi^{(1)}(\vec{x})$ pion field. $\vec{S}^{(1)}(\vec{x})$ represents a pseudo-vector iso-scalar field ((1)-component) with a pronounced dipole shape. The divergence is the according pseudo-scalar iso-vector source density. One should note that the structure of the intrinsic state extends over the whole nucleus and is hence of long range.

All other spin-isospin densities are two orders of magnitude smaller which means zero within numerical uncertainty and hence not displayed. One should keep in

mind that the intrinsic state $|Q; +\rangle$ can be rotated in isospin space around the (3)-axis resulting only in an overall phase of the ground state, because the intrinsic state is projected on good charge number by summing up rotations around the (3)-axis, cf. Eq. (6). Likewise one can rotate the intrinsic state in coordinate space without affecting the angular momentum projected 0^+ ground state, so that the dipole in y -direction could also point in any other direction.

Let us try to explain the physical meaning of the non-zero intrinsic pseudo-scalar isovector source density $\vec{\nabla} \cdot \vec{S}^{(1)}(\vec{x})$ with help of an analogy to the Coulomb interaction. Consider a positronium, negatively charged electron plus positively charged positron, in their atomic ground state. This state has angular momentum zero and the probability to find a positron at some position equals that of the electron. Hence the mean value or expectation value of the charge density ρ_e is zero and consequently there is no Coulomb field Φ_e which of course must not be interpreted that there is no Coulomb attraction. But if we take a ‘‘snap shot’’ we find the positron and electron on opposite sides (perfect correlation) forming a dipole with non-zero charge density and non-zero Coulomb field by which they attract each other. After projecting this dipole on a 0^+ state we get the true positronium ground state.

Looking at Eq. (25) and replacing

$$\begin{aligned}\Phi_\pi^{(i)} &\rightarrow \Phi_e \\ \frac{g_\pi}{M} \vec{\nabla} \cdot \vec{S}^{(i)} &\rightarrow 4\pi\rho_e \\ m_\pi &\rightarrow 0\end{aligned}$$

one recovers the well known equation for a Coulomb field created by a charge density. The analogy is obvious, the intrinsic state is the ‘‘snap shot’’ where one sees the dipole like source density as a one-body mean field (Fig. 3). If one wants to see that correlation in the spherical quantum state with good parity one would have to resort to two-body information or correlation functions, cf. Fig. (2) in Ref. [6].

C. Phenomenological interaction

In Refs. [9, 10, 11, 12, 13] Ikeda, Sugimoto and Toki propose the idea to mix proton and neutron wave function at the single-particle level and then perform charge and parity projection of the many-body state. They use for the 4 single-particle states for ${}^4\text{He}$ ($\nu = 1, 2; m = \pm 1/2$)

$$\langle \vec{x} | \nu, \frac{1}{2}m \rangle = \sum_{\substack{m_t=p,n \\ l=0,1}} \phi_{\nu,lm_t}(x) [Y^l(\theta, \phi) | \frac{1}{2} \rangle]_{\frac{1}{2}m} \otimes |m_t\rangle. \quad (32)$$

Here, the spatial part of the wave function contains s - and p -wave components by construction, and the radial part ϕ_{ν,lm_t} is expanded in terms of Gaussian functions.

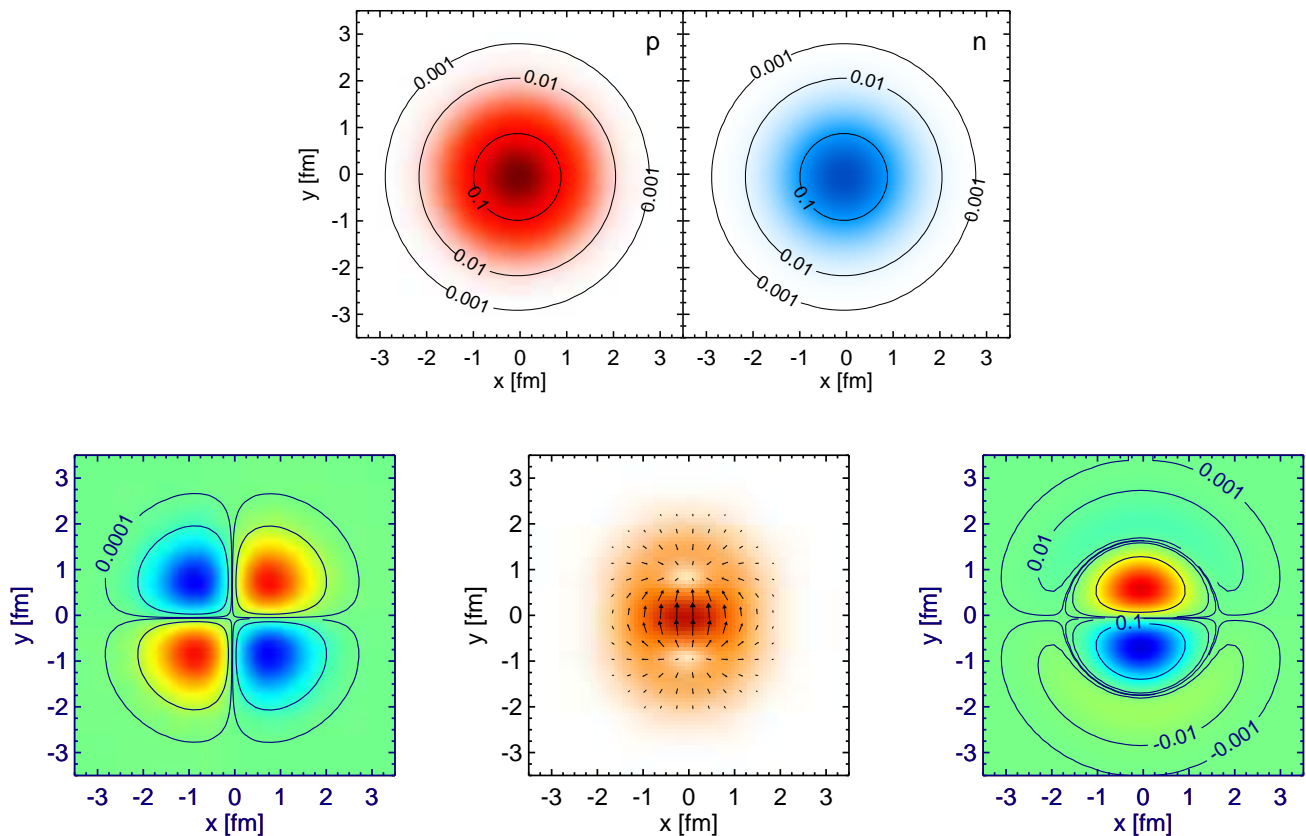


FIG. 3: (Color online) Densities calculated with parity projected intrinsic state $|Q; +\rangle$ obtained for $I_\vartheta = 0.09 \text{ fm}^3$. Upper panel: proton density $\rho_p(\vec{x})$ and neutron density $\rho_n(\vec{x})$ (in fm^{-3}); lower panel: isospin density $\rho_r^{(1)}(\vec{x})$ (in fm^{-3}); spin-isospin density $\vec{S}^{(1)}(\vec{x})$; divergence of spin-isospin density $\vec{\nabla} \cdot \vec{S}^{(1)}(\vec{x})$ (in fm^{-4}). Contour lines in decades.

A phenomenological interaction that is composed of a central Volkov potential [41] and the tensor plus spin-orbit G3RS force [42] is used. It is argued that the mixing of parity and isospin is able to account for appropriate tensor correlations in the α -particle when the triplet-even component of the central part is reduced by 0.81 and the $\mathcal{T}_i\mathcal{T}_j$ part of the tensor force enhanced by a factor 1.5. For this special interaction, which we will refer to as Sugimoto-Ikeda-Toki (SIT) interaction, the expectation value of the tensor potential amounts to -30 MeV and the L=2 admixture to 7.3 % in their 4-body state.

Using the FMD basis with two Gaussians per nucleon, in order to allow for a p -wave component in the single-particle wave function, we obtain the results presented in Table III, which correspond approximately to those in Ref. [12]. But the tensor contribution in the FMD state is 4.5 MeV larger and the ground state is by 7.25 MeV more bound, which means that the FMD state is a better variational state and represents more tensor correlations. In contrast to that, as seen in section III A, the phase-shift equivalent and in this sense realistic potential V_{UCOM} leads typically to only -5 MeV tensor contribution with the same type of FMD trial state.

TABLE III: Comparison of expectation values of the Hamiltonian, the intrinsic kinetic energy, the total potential energy (Coulomb included) and the tensor potential when using the trial states of Ref. [12], charge and parity projected FMD and an exact calculation. For all cases the SIT-potential [12] is employed. Numerical values are in MeV.

	Ref. [12]	FMD-CPP	Exact
$\langle \tilde{H} \rangle$	-28.19	-35.44	-121.77
$\langle \tilde{T} \rangle$	64.39	63.78	150.56
$\langle \tilde{V} \rangle$	-92.58	-99.22	-272.33
$\langle \tilde{V}_T \rangle$	-30.59	-35.19	-207.08

This suggests that the SIT-potential has an unrealistic ratio of tensor to central potential. To investigate that further we perform an exact calculation using an HH expansion and a Lee-Suzuki transformation to accelerate convergence, as proposed in [43]. The exact results shown in Table III exhibit a dramatic overbinding with the SIT-potential. The reason is that the tensor potential

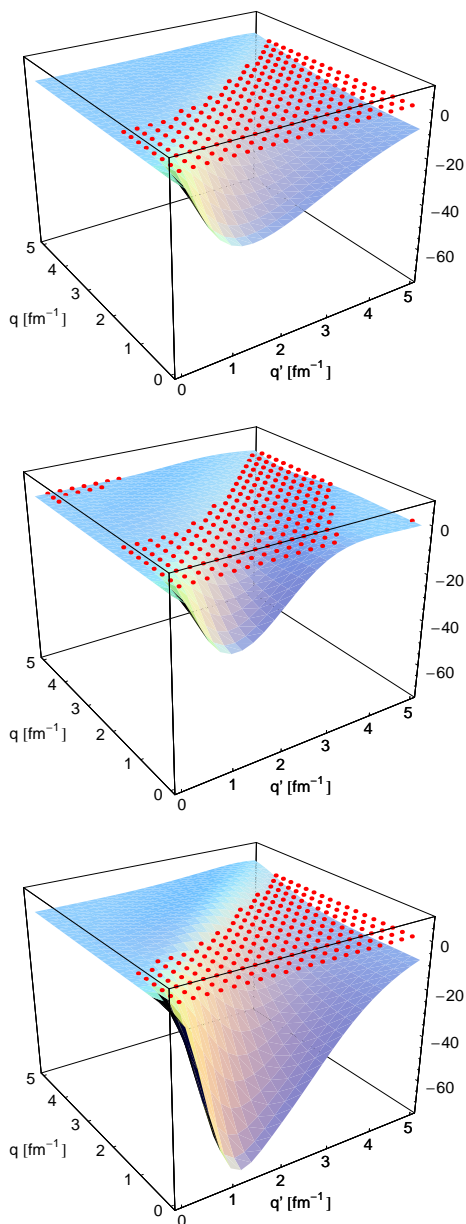


FIG. 4: (Color online) Off-diagonal momentum space matrix elements (in MeV fm^3) of the initial AV18 potential (top), the V_{UCOM} potential for $I_\vartheta = 0.09 \text{ fm}^3$ (center), and the SIT-potential (bottom) between the 3S_1 and 3D_1 channel. Dotted plane indicates 0 MeV fm^3

gives a completely unrealistic contribution of -207 MeV . Thus neither the FMD nor the trial state of Ref. [12] can represent in a reliable way the huge tensor correlations induced by the unrealistic phenomenological tensor part of the SIT-interaction.

The reason for the large difference between the FMD or the Sugimoto *et al.* results [12] and the exact result becomes understandable when looking at Fig. 4, where the non-diagonal momentum space matrix ele-

ments of the AV18 potential, the corresponding V_{UCOM} for $I_\vartheta = 0.09 \text{ fm}^3$, and the SIT potential between the 3S_1 and 3D_1 channel, that is sensitive to the tensor force only, are displayed. The off-diagonal matrix elements of the initial interaction are strongly reduced for $q' \gtrsim 2 \text{ fm}^{-1}$ by the UCOM transformation [8]. In contrast to that the SIT matrix elements are not only much larger than those of V_{UCOM} but even larger than those of the AV18 interaction and the SIT interaction connects low momenta with momenta high above the Fermi momentum. Those high momentum components above about 2 fm^{-1} are not present in a low-momentum basis consisting of a few Slater determinants and thus the according correlations or admixtures cannot be represented. On the other side the exact HH state includes high momenta and thus can accommodate the correlations caused by this part of the potential. This explains the drastic differences seen in the energies.

The SIT-interaction is an example that fitting a phenomenological potential to a specific nucleus without reference to realistic interactions can lead to unstable and unpredictable results and does not allow to draw definitive conclusions on tensor correlations in nuclei. States that live in a too small Hilbert space are forced by too strong interactions to produce the desired kind of correlations. Ikeda, Sugimoto and Toki are aware of this problem and argue in some of their papers with the strength of the G-matrix [10, 12, 13]. But as V_{UCOM} plays the same role as a G-matrix we believe that the long range tensor correlations can only partly be represented by a charge and parity projected intrinsic Slater determinant, as shown in Sec. III A.

D. Time reversal symmetry

In this section we would like to make a remark about time reversal symmetry [44] of our charge and parity projected FMD state. With the charge and parity projection we actually create intrinsic states which are not invariant under time reversal. Since the variational single-particle parameters are complex they may get a non-zero imaginary part, violating the time reversal symmetry. In order to restore the symmetry, we generate a time reversal symmetric state by

$$|\Psi\rangle = \tilde{P}_{CM} \tilde{P}_{MK}^J \tilde{P}_{\pi}^{\pi} \tilde{P}_{M_T}^{M_T} (e^{i\phi}|Q\rangle + e^{-i\phi}|\bar{Q}\rangle), \quad (33)$$

where $|\bar{Q}\rangle = \mathcal{T}|Q\rangle$, is the time reversed Slater determinant. Then we minimize the energy with respect to the phase ϕ ;

$$E_0 = \min_{\{\phi\}} \frac{\langle \Psi | H | \Psi \rangle}{\langle \Psi | \Psi \rangle}. \quad (34)$$

We find that for the investigated cases the effect of the symmetry restoration is at most of the order of 100 keV and thus negligible for the purpose of this paper.

IV. CONCLUSIONS

Within Fermionic Molecular Dynamics the effects of mixing proton and neutron components of the single-particle states of a single Slater determinant are investigated. For that we perform for ${}^4\text{He}$ variational calculations by minimizing the energy of the charge and parity projected Slater determinant using realistic nucleon-nucleon interactions. It turns out that the variation needs to be performed after charge and parity projection in order to obtain a non-vanishing tensor contribution to the ground state energy of the doubly magic nucleus ${}^4\text{He}$. The intrinsic state that is not yet charge projected features a non-vanishing pseudo-vector iso-scalar spin-isospin density that is intimately related to the pseudo-scalar iso-vector pion fields which are responsible for the long range part of the tensor force.

A Hartree-Fock type variation without projection does not break charge and parity of the single-particle states and hence the expectation value of the tensor interaction is zero.

The extra correlation energy obtained by the new degrees of freedom that mix charge turns out to be small for realistic interactions, smaller than anticipated from

earlier work by Sugimoto, Ikeda and Toki. The main reason is that they did not use a realistic interaction but adopted a tensor force that scatters to high momenta and at low momenta is about twice the strength of the tensor part in V_{UCOM} .

Our result is that charge mixing and parity breaking of one-body states can account only for a fraction of the long range correlation energy missing in a mean-field picture (single Slater determinant). One should however keep in mind that ${}^4\text{He}$ is the most demanding nucleus in this respect. Even if the additional energy due to long range correlations is found to be small here, we cannot extrapolate this result to open shell nuclei. Also a variation after angular momentum projection might change the situation. These issues will be subject of future investigations.

Acknowledgments

One of the authors (S.B.) would like to thank S. Quaglioni for useful discussion about the no-core shell model. We are grateful to P. Navrátil and N. Barnea for providing us with the NCSM and HH codes, respectively.

-
- [1] D. R. Entem and R. Machleidt, *Phys. Rev. C* **68**, 041001(R) (2003).
- [2] E. Epelbaum, *Prog. Part. Nucl. Phys.* **57**, 654 (2006).
- [3] R. B. Wiringa, V. G. J. Stoks, and R. Schiavilla, *Phys. Rev. C* **51**, 38 (1995).
- [4] P. Navrátil and B. R. Barrett, *Phys. Rev. C* **54**, 2986 (1996).
- [5] H. Feldmeier, T. Neff, R. Roth, and J. Schnack, *Nucl. Phys.* **A632**, 61 (1998).
- [6] T. Neff and H. Feldmeier, *Nucl. Phys.* **A713**, 311 (2003).
- [7] R. Roth, T. Neff, H. Hergert, and H. Feldmeier, *Nucl. Phys.* **A745**, 3 (2004).
- [8] R. Roth, H. Hergert, P. Papakonstantinou, T. Neff, and H. Feldmeier, *Phys. Rev. C* **72**, 034002 (2005).
- [9] S. Sugimoto, H. Toki, and K. Ikeda, *Nucl. Phys.* **A721**, 669c (2003).
- [10] K. Ikeda, S. Sugimoto, and H. Toki, *Nucl. Phys.* **A738**, 73 (2004).
- [11] S. Sugimoto, K. Ikeda, and H. Toki, *Nucl. Phys.* **A738**, 240 (2004).
- [12] S. Sugimoto, K. Ikeda, and H. Toki, *Nucl. Phys.* **A740**, 77 (2004).
- [13] S. Sugimoto, K. Ikeda, and H. Toki, *Nucl. Phys.* **A789**, 155 (2007).
- [14] H. Feldmeier, in *The Nuclear Equation of State*, eds. W. Greiner and H. Stöcker, (1989) Plenum Press, New York, NATO ASI Series B: Physics, Vol. **216A**, p. 375
- [15] H. Feldmeier and J. Schnack, *Rev. Mod. Phys.* **72**, 655 (2000).
- [16] T. Neff and H. Feldmeier, *Nucl. Phys.* **A738**, 357 (2004).
- [17] T. Neff, H. Feldmeier and R. Roth, *Nucl. Phys.* **A752**, 321 (2005).
- [18] T. Neff and H. Feldmeier, *Eur. Phys. J. Special Topics* **156**, 69 (2008)
- [19] H. Feldmeier and T. Neff, *Proc. International School of Physics “Enrico Fermi” Course CLXIX “Nuclear Structure far from Stability: New Physics and new Technology”* edited by A. Covello, F. Iachello, R.A. Ricci, and G. Maino (2008)
- [20] Y. Kanada-En’yo and H. Horiuchi, *Prog. Theor. Phys. Suppl.* **142**, 205 (2001).
- [21] R. Roth, P. Papakonstantinou, N. Paar, H. Hergert, T. Neff, and H. Feldmeier, *Phys. Rev. C* **73**, 044312 (2006).
- [22] M. Chernykh, H. Feldmeier, T. Neff, P. von Neumann-Cosel, and A. Richter, *Phys. Rev. Lett.* **98**, 032501 (2007).
- [23] W. E. Ormand, D. J. Dean, C. W. Johnson, G. H. Lang, and S. E. Koonin, *Phys. Rev. C* **49**, 1422 (1994).
- [24] N. Paar, P. Papakonstantinou, H. Hergert, and R. Roth, *Phys. Rev. C* **74**, 014318 (2006).
- [25] C. Barbieri, *Phys. Lett.* **B643**, 268 (2006).
- [26] S. Bacca, *Phys. Rev. C* **75**, 044001 (2007).
- [27] A. Nogga, S. K. Bogner, A. Schwenk, *Phys. Rev. C* **70** 061002(R) (2004).
- [28] H. Kamada, A. Nogga, W. Glöckle, E. Hiyama, M. Kamimura, K. Varga, Y. Suzuki, M. Viviani, A. Kievsky, S. Rosati, J. Carlson, S. C. Pieper, R. B. Wiringa, P. Navrátil, B. R. Barrett, N. Barnea, W. Leidemann, and G. Orlandini, *Phys. Rev. C* **64**, 044001 (2001).
- [29] P. Navrátil, G. P. Kamuntavičius, and B. R. Barrett, *Phys. Rev. C* **61**, 044001 (2000).
- [30] N. Barnea and A. Novoselsky, *Ann. Phys. (N.Y.)* **256**, 192 (1997); N. Barnea and A. Novoselsky, *Phys. Rev. A* **57**, 48 (1998).

- [31] N. Barnea, Phys. Rev. A **59**, 1135 (1999).
- [32] D. Gazit, S. Bacca, N. Barnea, W. Leidemann, and G. Orlandini, Phys. Rev. Lett. **96**, 112301 (2006).
- [33] D. Gazit, N. Barnea, S. Bacca, W. Leidemann and G. Orlandini, Phys. Rev. C **74**, 061001(R) (2006).
- [34] S. Bacca, M. A. Marchisio, N. Barnea, W. Leidemann and G. Orlandini, Phys. Rev. Lett. **89**, 052502 (2002).
- [35] S. Bacca, N. Barnea, W. Leidemann and G. Orlandini, Phys. Rev. C **69**, 057001 (2004).
- [36] S. Bacca, H. Arenhövel, N. Barnea, W. Leidemann and G. Orlandini, Phys. Lett. **B603**, 159 (2004).
- [37] S. Bacca, H. Arenhövel, N. Barnea, W. Leidemann and G. Orlandini, Phys. Rev. C **76**, 014003 (2007).
- [38] D. Gazit, arXiv:0803.0036v2 and references therein.
- [39] N. Barnea, W. Leidemann, and G. Orlandini, Phys. Rev. C **74**, 034003 (2006).
- [40] I. Stetcu, S. Quaglioni, S. Bacca, B. R. Barrett, C. W. Johnson, P. Navrátil, N. Barnea, W. Leidemann, and G. Orlandini. Nucl. Phys. **A785**, 307 (2007).
- [41] A. B. Volkov, Nucl. Phys. **74** 33 (1965).
- [42] R. Tamagaki, Prog. Theor. Phys. **39**, 91 (1968).
- [43] N. Barnea, W. Leidemann, and G. Orlandini, Phys. Rev. C **61**, 054001 (2000); Nucl. Phys. **A693**, 565 (2001).
- [44] A. Bohr and B. R. Mottelson, *Nuclear Structure*, Vol. 1, World Scientific Publishing, Singapore, 1999.